Mon. Not. R. Astron. Soc. **000**, 1–**??** (2011) Printed 20 January 2013 (MN LaTeX style file v2.2)

arXiv:1104.5460v1 [astro-ph.CO] 28 Apr 2011

Analyzing derived metallicities and ionization parameters from model-based determinations in ionized gaseous nebulae

O. L. Dors Jr.[1]⋆, Angela Krabbe[1], Guillermo F. Hägele[2,3], Enrique Pérez-Montero[4]
[1] *Universidade do Vale do Paraíba, Av. Shishima Hifumi, 2911, Cep 12244-000, São José dos Campos, SP, Brazil*
[2] *Facultad de Ciencias Astronómicas y Geofísicas, Universidad Nacional de la La Plata, Paseo del Bosque s/n, 1900 La Plata, Argentina.*
[3] *Departamento de Física Teórica, C-XI, Universidad Autónoma de Madrid, 28049 Madrid, Spain.*
[4] *Instituto de Astrofśica de Andalucúa (CSIC), PO Box 3004, 18080 Granada, Spain*

Accepted -. Received -.

ABSTRACT

We analyze the reliability of oxygen abundances and ionization parameters obtained from different diagnostic diagrams. For this, we compiled from the literature observational emission line intensities and oxygen abundance of 446 star-forming regions whose O/H abundance was determined by direct estimation of electron temperature. The abundances compiled were compared with the values calculated in this work using different diagnostic diagrams in combination with results from a grid of photoionization models. We found that the [O III]/[O II] vs. [N II]/[O II], [O III]/Hβ vs. [N II]/[O II], and ([O III]/Hβ)/([N II]/Hα) vs. [S II]/[S III] diagnostic diagrams give O/H values close to the $T_{\rm e}$-method, with differences of about 0.04 dex and dispersion of about 0.3 dex. Similar results were obtained by detailed models but with a dispersion of 0.08 dex. The origin of the dispersion found in the use of diagnostic diagrams is probably due to differences between the real N/O-O/H relation of the sample and the one assumed in the models. This is confirmed by the use of detailed models that do not have a fixed N/O-O/H relation. We found no correlation between ionization parameter and the metallicity for the objects of our sample. We conclude that the combination of two line ratio predicted by photoionization models, one sensitive to the metallicity and another sensitive to the ionization parameter, which takes into account the physical conditions of star-forming regions, gives O/H estimates close to the values derived using direct detections of electron temperatures.

Key words: galaxies: general – galaxies: evolution – galaxies: abundances – galaxies: formation– galaxies: ISM

1 INTRODUCTION

Oxygen abundance estimates in star-forming regions play a crucial role in the understanding of galaxy evolution. For example, oxygen radial gradients in spiral galaxies obtained by H II region observations (e.g. Stanghellini et al. 2010; Kewley et al. 2010; Bresolin et al. 2009; Krabbe et al. 2008; Dors & Copetti 2005; Kennicutt et al. 2003) are essential to test chemical evolution models (see Mollá & Díaz 2005) and to investigate the effect of environment on galaxy interactions (Ellison et al. 2010; Dors & Copetti 2006; Skillman et al. 1996) as well as the mass-metallicity relation of galaxies (e.g. Pilyugin et al. 2004; Pérez-Montero & Contini 2009). Likewise, oxygen abundance estimates in metal-poor galaxies are also important to test theories of chemical evolution of galaxies because these are the least chemically evolved objects (Kunth & Sargent 1983).

Unfortunately, for the most of star-forming regions, only collisionally excited emission-lines (CELs) in the optical are bright enough to be used for the derivation of elemental abundance. CELs are temperature sensitive, thus, only an accurate determination of the metallicity can be achieved from the previous estimation of the electron temperature (this method will be called $T_{\rm e}$-method) using, for instance, the ratio of different CELs [O III](λ4959 + λ5007)/λ4363 which are weak or unobservable in star-forming regions with high metallicity and/or low excitation (Dors et al. 2008; Díaz et al. 2007). In these cases, oxygen abundances can be obtained by empirical (i.e. using oxygen determinations via $T_{\rm e}$-method) or theoretical (i.e. using photoionization models) calibrations between oxygen abundances and more easily measured line ratios (hereafter strong-line methods). The oxygen abundance indicator R_{23}=([O II]λ3727+[O III]λ4959,λ5007)/Hβ proposed by Pagel et al. (1979) has found large acceptance in this context and several authors have calibrated this line ratio with O/H abundance (e.g. Edmunds & Pagel 1984; Dopita & Evans 1986; Pilyugin 2001; Dors & Copetti 2005; among others). Additional O/H indicators based on other emission lines such as N_2=[N II]λ6584/Hα (Storchi-Bergmann et al. 1994), [N II]λ6584/[O III]λ5007 (Alloin et al. 1979),

---

⋆ E-mail:olidors@univap.br

S_{23}=([S II]$\lambda\lambda$6716,6731+[S II]$\lambda\lambda$9069,9532)/Hβ (Vílchez & Esteban 1996; Díaz & Pérez-Montero 2000) have also been suggested (see also Kewley & Dopita 2002). However, distinct methods or distinct calibrations of a same oxygen indicator provide different oxygen values with discrepancies up to 1.0 dex (Kewley & Ellison 2008; Rupke et al. 2008; Dors & Copetti 2005; Kennicutt et al. 2003). Currently, the large number of direct oxygen estimates available in the literature have helped to investigate this discrepancy. For example, Yin et al. (2007) determined the gas-phase oxygen abundance for a sample of 695 galaxies and H II regions using the T_e-method and compared these determinations with the ones via R_{23}, N_2, ([N II]λ6584/Hα)/([O III]λ5007/Hβ), and [S II](λ6717+λ6731)/Hα. They found that among the indices above, the N_2 provides more consistent O/H abundances when compared with the ones via T_e-method. Similar analysis was also done by Pérez-Montero & Díaz (2005), Liang et al. (2006), and Nagao et al. (2006).

The studies above analyzed strong-line methods based mainly on one line ratio, such as the R_{23}, N_2, among others. In principle, the use of diagnostic diagrams, suggested by Baldwin et al. (1981) to separate objects according to their primary excitation mechanisms, containing line ratios strongly dependent on the degree of ionization and on the metallicity of star forming regions, can improve the accuracy of strong-line methods. Although a large number of these diagrams have been applied to estimate oxygen abundances and ionization parameters of star forming regions (e.g. Levesque et al. 2010, Viironen et al. 2007, Kewley et al. 2001, McGaugh et. al 1991, Dors et al. 2008, Dopita & Evans 1986), a comparison of oxygen estimates obtained from these diagrams and T_e-method is unavailable in the literature.

Another important issue related with the determination of metallicity using strong-line methods is the relation between the ionization parameter and the metallicity, which is still controversial. For example, Garnett et al. (1997), in a study of the interstellar abundance gradient in NGC 2403 found that any correlation between ionization parameter and abundance must be a weak one. This result is in agreement with that obtained by Kennicutt & Garnett (1996) from measurements of the [S II]/[S III] ratio in 41 H II regions in M101 and with the one found for three barred galaxies established by Dors & Copetti (2005). On the other hand, Bresolin et al. (1999) found that in metal poor disk H II regions the ionization parameter is about 4 times larger than in H II regions with solar metallicity. This relation was also found by Maier et al. (2006) and Nagao et al. (2006) for a sample of galaxies. This subject is important to study the association of the mass-metallicity relation with the mass-age relation in local galaxies or the relation between gas metallicity and stellar metallicity (Nagao et al. 2006). Additional analysis using several methods would help to solve this disagreement.

In this paper, we employed a grid of photoionization models and data compiled from the literature in order to estimate the oxygen abundance using diagnostic diagrams to compare with those via T_e-method, as well as to investigate the relation of the ionization parameter with the metallicity. Detailed photoionization models are also built to produce more precise determinations of these parameters. In Section 2, we describe the observational data used in the analysis. The modeling procedures are presented in Sect. 3. A description of the diagnostic diagrams employed is given in Sect. 4. The results and discussion are presented in Sects. 5 and 6, respectively. A conclusion of the outcome is given in Sect. 7.

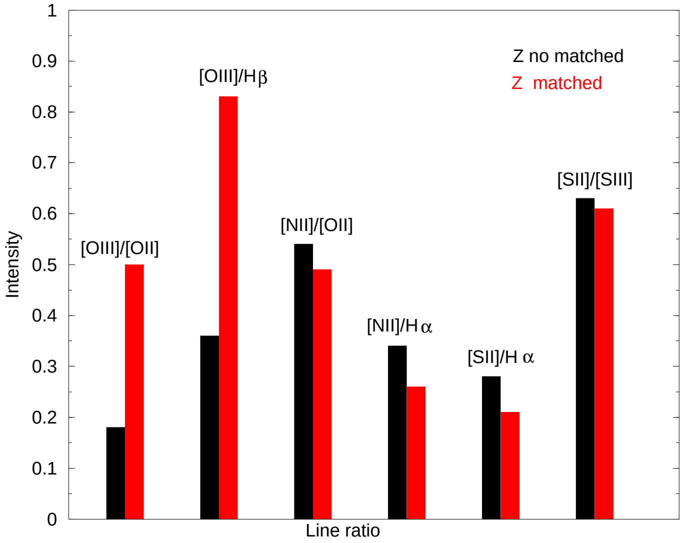

Figure 1. Comparison of some predicted line ratio intensities from photoionization models with nebular and stellar metallicity matched (red) and no matched (black).

Table 1. Emission line ratios considered

Symbol	Definition
R_{23}	([O II]λ3727+[O III]λ4959,λ5007)/Hβ
[O III]/Hβ	[O III]λ5007/Hβ
[O III]/[O II]	[O III]λ5007/[O II]λ3727
[N II]/Hα	[N II]λ6584/Hα
[N II]/[O II]	[N II]λ6584/[O II]λ3727
[S II]Hα	([S II]λ6716+λ6731)/Hα
[S II]/[S III]	([S II]λ6716+λ6731)/([S III] λ9069+λ9532)

2 OBSERVATIONAL DATA

Observational emission line intensities of a sample of H II galaxies and H II regions and the oxygen abundance computed using the T_e-method were compiled from literature.

The emission lines considered in our analysis are listed in Table 1. This compilation includes data of H II regions obtained by Bresolin et al. (2009), Bresolin et al. (2005), Bresolin et al. (2004), Bresolin (2007), Lee & Skillman (2004), and Kennicutt et al. (2003). The data on H II galaxies were obtained by Izotov et al. (2006), Lee et al. (2004), Izotov & Thuan (2004), Vílchez & Iglesias-Páramo (2003), Hägele et al. (2008), and Guseva et al. (2000). The sample consists of 446 objects (86 H II regions and 360 H II galaxies) whose O/H abundance are in the range $7.0 < 12 + \log(\mathrm{O/H})_{T_e} < 9.0$ and represents practically the entire metallicity range of star-forming regions (see Pilyugin et al. 2004a). The objects of the sample have $z < 0.07$ and measurements corrected by dust extinction and no AGN and gas shock contributions are present in their ionization.

3 PHOTOIONIZATION MODELS

3.1 Model Grid

To enable the estimation of the oxygen abundance and the ionization parameter using diagnostic diagrams, we employed the pho-

Table 2. Final parameters of the detailed photoionization models for H II regions observed by Kennicutt et al. (2003)

H II region	12+log(O/H)	log(N/O)	log(S/O)	log U	N_e (cm^{-3})	Age (Myr)
H 1013	8.48	-0.72	-1.34	-1.94	47	2.5
H 1105	8.71	-1.06	-1.64	-2.35	248	1.0
H 1159	8.80	-1.28	-1.94	-2.55	5	1.0
H 1170	8.07	-0.83	-1.31	-2.60	9	2.5
H 1176	8.16	-0.76	-1.38	-2.05	33	2.5
H 1216	8.00	-1.28	-1.64	-2.52	33	1.0
H 336	8.75	-0.80	-1.58	-2.68	15	2.5
H 409	8.53	-1.15	-1.58	-2.37	213	1.0
H 67	8.00	-1.15	-1.64	-2.82	10	2.5
N 5471-D	8.10	-1.15	-1.64	-2.4	110	2.5
S DH323	7.76	-1.45	-1.61	-2.91	61	2.5

Table 3. Observed intensity lines and those predicted by our detailed models

H II region	[O II]λ3727		[O III]λ4363		[O III]λ5007		[N II]λ6584		[S II]λ6720		[S III]λ9069 + λ9532	
	Obs.	Mod.	Obs.	Mod.	Obs.	Mod.	Obs.	Mod.	Obs.	Mod.	Obs.	Mod.
H 1013	188±10	185	—	0.20	103±5	105	64.6±3.4	67	28.8±1.1	26	131.6±7.0	171
H 1105	185±10	188	1.4±0.1	0.74	316±17	317	33.4±1.8	34	24.1±0.9	27	126.6±11	139
H 1159	198±10	194	1.9±0.4	0.63	317±17	316	23.6±1.3	25	29.8±1.1	27	97.0 ±5.5	66
H 1170	308±16	295	1.6±0.2	1.67	201±11	194	44.0±2.3	41	56.7±2.1	51	170.0±9.3	136
H 1176	160±8	153	2.4±0.3	2.74	369±20	357	21.2±1.1	23	23.0±0.8	19	113.5±6.1	137
H 1216	151±8	149	4.7±0.3	6.67	473±25	478	11.0±0.6	9	18.9±0.7	18	83.0±4.6	63
H 336	178±9	183	—	0.02	23±1	26	95.9±5.1	99	56.8±2.1	58	107.0±5.7	102
H 409	218±12	212	2.3±0.2	1.39	370±20	359	27.3±1.4	24	31.2±1.1	28	90.1±4.9	141
H 67	244±13	248	3.5±0.5	4.67	342±18	356	16.3±0.9	19	26.3±1.3	29	92.1±5.7	62
N 5471-D	137±7	140	8.0±0.4	7.10	578±31	574	8.5±0.5	11	20.6±0.8	18	75.7±4.3	75
S DH323	194±10	198	5.5±0.9	3.7	227±12	234	7.9±0.7	7	20.8±1.4	23	—	42

toionization code Cloudy 8.00 (Ferland 2002) to build a grid of models covering a large space of nebular parameters. In these models, a stellar cluster was assumed to be responsible for the ionization of the nebulae, with a spectral energy distribution (SED) obtained using *Starburst*99 (Leitherer et al. 1999). We built models with stellar cluster formed by instantaneous burst with Salpeter initial mass function ($\alpha = -2.35$), lower and upper stellar mass limits of 0.1 $M_\odot$ and 100 $M_\odot$, respectively, and age of 2.5 Myr. Other papers that have considered stellar clusters as ionizing sources in order to reproduce strong forbidden lines of H II region (Dors & Copetti 2005; Dopita et al. 2000; Stasińska & Izotov 2003; Bresolin et al. 1999; Copetti et al. 1985) have derived about the same age for star-forming regions (i.e. 1-3 Myr). Similar ages have also been found from optical photometric data of giant H II regions (e.g. Mayya & Prabhu 1996). Selection effects may explain this limited range of ages. H II regions younger than about 1 Myr are difficult to be detected in the optical, because they are generally embedded in dusty molecular clouds which cause considerable optical extinction. Nebulae older than about 5 Myr are also difficult to be observed because their original massive stars have cooled or are dead (Dopita et al. 2000; García-Vargas et al. 1996; Copetti et al. 1985). We used the stellar evolution models from the Geneva group with high mass-loss rates and without stellar rotation (Meynet et al. 1994). The non-LTE atmosphere model of Pauldrach et al. (2001) was assumed in the models. If LTE atmosphere model is assumed instead of non-LTE model a lower ionization degree is produced in the hypothetical nebulae (Dors & Copetti 2003; Stasińska & Schaerer 1997). This would affect mainly ionization parameter rather than metallicity determinations via strong-line methods. The models were built having ionization parameter ranging from $\log U = -1.5$ to -3.5 (with a bin size of 0.5 dex), metallicities (traced by the oxygen abundance) Z= 0.04, 0.02, 0.008, 0.004, 0.001, plane-parallel geometry, and electron density of $N_e = 200$ cm^{-3}. This electron density value is typical of not evolved H II regions (Copetti et al. 2000).

The abundances of heavy metals in the nebula is scaled linearly to the solar metal composition through the comparison of the oxygen abundances, with the exception of the N abundance, which was taken from the relation log(N/O)=log(0.034+120 O/H) of Vila-Costas & Edmunds (1993). The solar composition (Z= 0.02) refers to Allende Prieto et al. (2001) and correspond to 12+log(O/H)= 8.69. The presence of internal dust was considered and the grain abundances (van Hoof et al. 2001) were also linearly scaled with the oxygen abundance. To take depletion of refractary elements onto dust grains into account the abundances of the elements Mg, Al, Ca, Fe, Ni, and Na were reduced by a factor of 10, and Si by a factor of 2 (Garnett et al. 1995) relative to the adopted abundances in each model.

The solar metallicity for the stars from the Geneva evolutionary tracks, which corresponds to the old solar oxygen abundance value [12+log(O/H)= 8.87 (Grevesse & Sauval 1998)], is higher than the value adopted for the nebular component. This produces

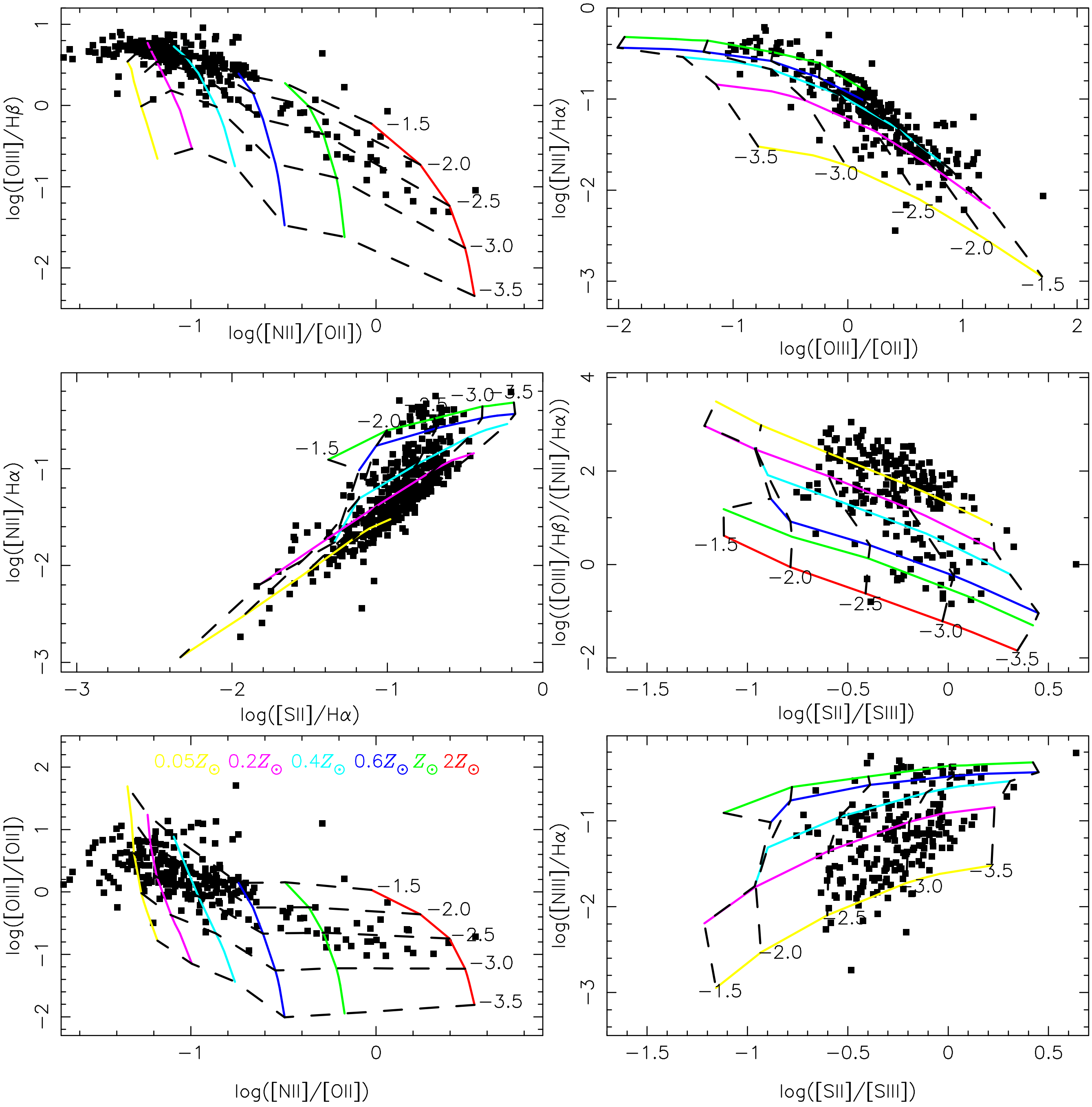

Figure 2. Diagnostic diagrams containing observational data taken from literature (see Sect. 2) and results of the grid of photoionization models (see Sect.3). The solid lines connect curves of iso-Z, while the dotted lines connect curves of iso-U. The values of $\log U$ and Z are indicated. Squares are the observational data. The line ratio used in each plot is defined in Table 1. The typical error bar (not shown) of the emission line ratio is about 10 %.

an imperfect match between gas and star metallicity in our photoionization models. As pointed out by Dopita et al. (2006), the main effect of this is that the computed stellar UV photon field result slightly softer. To investigate how this discrepancy affects our results, we built a model with a perfect match between nebular and stellar metallicities and compared the result with another model whose metallicities are in disagreement. This latter was built using a SED with 12+log(O/H)=8.69 obtained by linear interpolation of the spectra with Z= 0.02 and Z= 0.008. In Figure 1 we show the histogram with the comparison of some emission line intensities ratio predicted by these models. We can see that, with exception of [O III]/[O II] and [O III]/Hβ, the intensities of the majority of the line ratios show little variation when the stellar metallicity atmosphere change. Similarly, the predicted value of the R_{23} index (not shown in Fig. 1) shows a small deviation, i.e. about 12%, which corresponds to variations in the oxygen abundance from calibrations using this line ratio by only 0.02 dex. Thus, the disagreement between the nebular and stellar metallicity have little influence on the Z determinations from strong-line methods and can only affect U estimates in diagnostic diagrams which use the [O III]/[O II] and [O III]/Hβ. Interestingly, Dopita et al. (2006) found that critical line ratios changed by 0.1 dex or less, except for the [O I]λ6300/Hα ratio, when a test model with a 0.4 $Z_{\odot}$ spectral synthesis cluster model from *Starburst*99 embedded in a nebula with 1.0 $Z_{\odot}$ (12+log(O/H)= 8.66) is run. Along the paper the solar abundance adopted refers to 12+log(O/H)= 8.69 from Allende Prieto et al. (2001).

These models are similar to the ones of Dors & Copetti (2006) and have been successful in describing observational data of H II regions (see Dors et al. 2008; Krabbe et al. 2008, Krabbe et al. 2007).

3.2 Detailed models

In general, grids of photoionization models are built assuming a fixed N/O-O/H relation. However, this constancy can yield large uncertainties in O/H estimates via strong-line methods (Pérez-Montero & Contini 2009). This problem can be circumvented by the use of detailed photoionization models. To analyze the source of these uncertainties, we built detailed models in order to reproduce the observational emission line intensities of 11 H II regions (see Table 2) located along the disk of the galaxy M 101, observed by Kennicutt et al. (2003), and we compared our estimates with O/H and U values from other methods. These objects were selected because they cover the wide range in metallicity and ionization parameter considered in this paper. We computed individual models for each object adopting the following methodology. Firstly, a model for each region was built by initially guessing the Z and U values derived from a comparison between the grid of photoionization models shown in the diagnostic diagram [O III]/[O II] vs. [N II]/[O II] (see Figure 2) and the observational data. The electron density of each model was considered to be that computed utilizing the task temden of the package IRAF, where we consider the sulfur ratio [S II]λ6716/[S II]λ6731 and electron temperature for the O^{+} ion measured by Kennicutt et al. (2003). The stellar cluster was assumed to have an age of 2.5 Myr, $M_{\rm up}$ = 100 $M_{\odot}$ and metallicity was matched with the closest one nebular assumed in the models. Then, we ran new models ranging the O/H and U values by 0.3 and 0.5 dex, respectively, with a step of 0.1 dex. From this series of models we selected a model which produced the smallest $\sum\chi_i^2 = \chi^2_{[\rm O\,II]/H\beta} + \chi^2_{[\rm O\,III]/H\beta}$, where $\chi_i = (I^i_{\rm obs.} - I^i_{\rm pred.})^2/I^i_{\rm obs.}$; $I^i_{\rm obs.}$ and $I^i_{\rm pred.}$ are the observational and predicted intensities of the line ratios, respectively. Another series of models was computed considering the O/H and U values found by the criterion above but ranging the N/H and S/H abundances by 0.3 dex in order to reproduce the intensities of the [N II]λ6584 and [S II]λ6720 emission lines. The satisfactory solution is found when $I_{\rm pred.}$ reproduces $I_{\rm obs.}$ within the observational uncertainties and the model has the smallest $\sum\chi_i^2 = \chi^2_{[\rm O\,II]/H\beta} + \chi^2_{[\rm O\,III]/H\beta} + \chi^2_{[\rm N\,II]/H\beta} + \chi^2_{[\rm S\,II]/H\beta}$. In some cases no satisfactory solution was reached considering the age of the ionizing cluster of 2.5 Myr. For these, it was necessary to assume an age of 1 Myr because their observed emission lines could only be reproduced by means of a harder spectral energy distribution. In Table 2, we present the final parameter obtained for the models.

4 DIAGNOSTIC DIAGRAMS

We employ six diagnostic diagrams containing predicted and observed emission line ratios sensitive to Z and U. The diagrams considered are described below.

- [O III]/[O II] vs. [N II]/[O II] — Diagnostic diagram suggested by Dopita et al. (2000), where the [O III]/[O II] has a strong dependence on U, on the effective temperature of the ionizing stars (e.g. Dors & Copetti 2003; Pérez-Montero & Díaz 2005) and on the metallicity (Kewley & Dopita 2002; Dopita et al. 2000). The [N II]/[O II] correlates strongly with Z above to $Z > 0.04$ $Z_{\odot}$ (Kewley & Dopita 2002), it is also dependent on the N/O abundance ratio (Pérez-Montero & Contini 2009) and it is almost independent of U (Kewley & Dopita 2002).

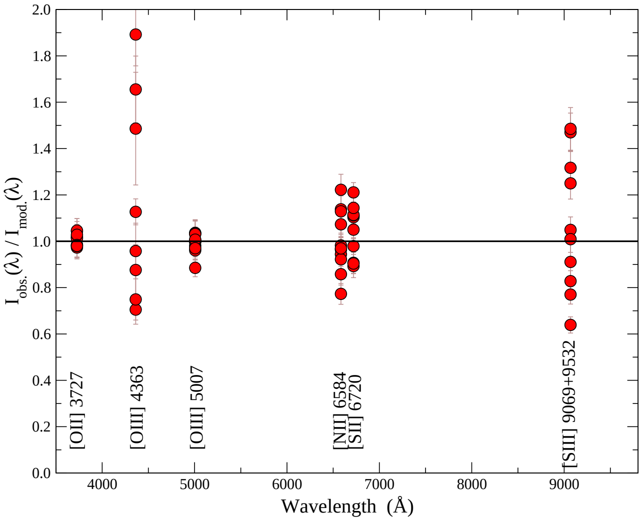

Figure 3. Ratio between observed and predicted emission line intensities of some H II regions located in M 101 observed by Kennicutt et al. (2003).

- [N II]/Hα vs. [S II]/Hα — This diagram was proposed by Viironen et al. (2007) to estimate the metallicity, where both line ratios are dependent on U and Z (Storchi-Bergmann et al. 1994; Kewley & Dopita 2002). Mazzuca et al. (2006) pointed out that the use of diagnostic diagrams using [N II]/Hα can yield degenerate values for Z, as star-forming regions with low Z and U have [N II]/Hα values similar to regions with high Z and U. In addition, no consistent values were found for oversolar abundances because the [N II]/Hα parameter saturates in this high-metallicity regime. Therefore, we did not consider models with metallicity over-solar. For the [S II]/Hα, this line ratio is strongly dependent on U and increases with the abundance for low metallicities (Levesque et al. 2010).
- [O III]/Hβ vs. [N II]/[O II] — Diagram proposed by Dopita et al. (2000). The [O III]/Hβ was suggested by Edmunds & Pagel (1984) as an O/H indicator. However, due to its dependence on U (Dopita & Evans 1986; McGaugh et. al 1991) a combination with another line ratio is preferable, otherwise, crude O/H estimates with uncertainties of about 0.5 dex are produced (Kobulnicky et al. 1999).
- [N II]/Hα vs. [S II]/[S III] — The [S II]/[S III] was proposed to be a U indicator by Díaz et al. (1991) for moderate to high metallicity regime (see also Dopita & Evans 1986), and it has little dependence on Z. The problem in using this line ratio is that it is underestimated by photoionization models (Garnett 1989), especially for high metallicity (Dors & Copetti 2005) doing any estimation in this regime is somewhat uncertain.
- ([O III]/Hβ)/([N II]/Hα) vs. [S II]/[S III] — Pettini & Pagel (2004) showed that ([O III]/Hβ)/([N II]/Hα) is dependent on Z. Because this line ratio is also dependent on U, we combined it with the [S II]/[S III] in order to minimize the uncertainties in Z determinations.

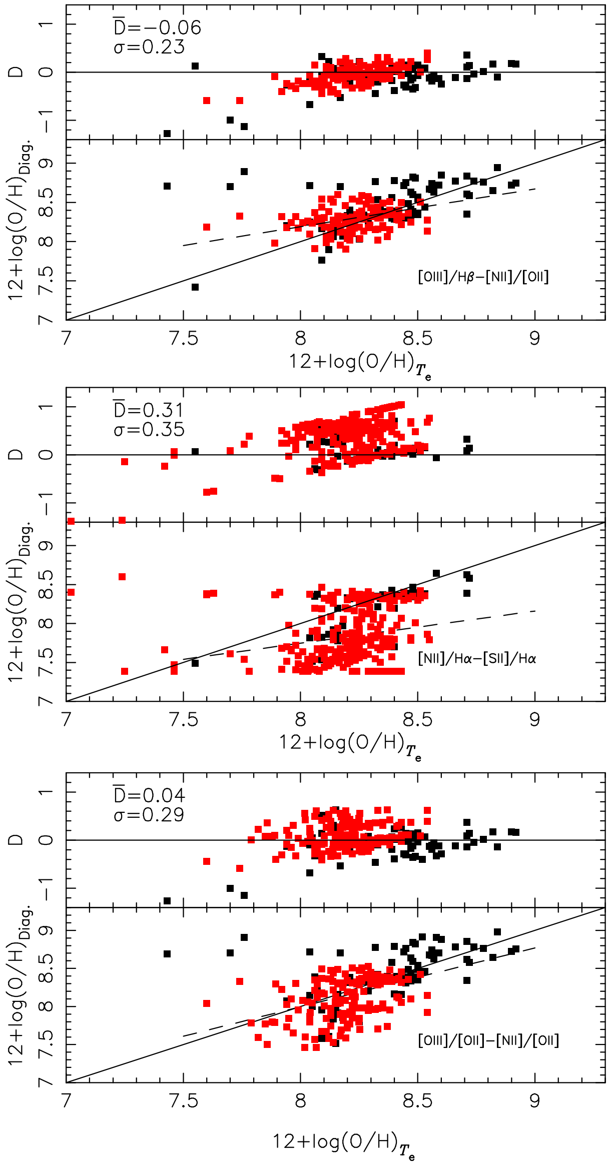

Figure 4. Comparison between the oxygen abundances derived using the $T_{\rm e}$-method with those computed using the diagnostic diagrams. In each plot the diagnostic diagrams used to compute the oxygen abundance are indicated. The top panel of each diagram shows the difference between oxygen abundance via $T_{\rm e}$-method and via diagnostic diagrams. The average value of this difference and the dispersion are shown in each plot. Solid lines represent the equality of the two estimates. The results for H II galaxies and H II regions are marked by red and black points, respectively

- [N II]/Hα vs. [O III]/[O II] — We investigate the combination between these line ratios to eliminate the problem existing with the use of [S II]/[S III].

5 RESULTS

In Figure 2, the diagnostic diagrams described above containing the results of our grid of photoionization models and the data sample is shown. The majority of the observational data fall within the regions occupied by the models. However, in the diagram [O III]/Hβ vs. [N II]/[O II] the models predict [O III]/Hβ values lower than the observed ones for the low metallicity regime and high U values, result also found for the ([O III]/Hβ)/([N II]/Hα) line ratio. Similar difficulty in modeling metal poor star-forming regions have been found by other authors. For example, Dopita et al. (2006), who used the same SEDs used in this paper, found that their models do not reproduce the observed emission line diagnostic ratios of objects with $Z < 0.4\,Z_{\odot}$. Martín-Manjón et al. (2008), using a combination of photoionization models and sets of stellar yields from Gavilán et al. (2005), also found that their models do not reproduce observational data of most metal deficient H II galaxies (see also Fernandes et al. 2003). Kewley et al. (2001) pointed out that this disagreement is due to that stellar ionizing spectra are not hard enough in the far ultraviolet region, and inclusion of the effects of continuum metal opacities in stellar atmospheres should be a way of improving the models accuracy. However, in our work we adopted stellar atmosphere models of Pauldrach et al. (2001), which include treatments of continuum metal opacities, and still this disagreement can be noted. A solution for this problem seems to include the effects of rotation in stellar models (see discussion above). The number of points ranges in the diagrams because for some data set no all emission lines considered were observed. For example, in Izotov et al. (2006) the [O II]λ3727 is not observed in 30% of the objects.

For the detailed models, a comparison of the predicted and observed emission line intensities is listed in Table 3, and Fig. 3 shows the ratio between these. We can see that the models reproduce very well (with differences lower than ~ 15 %) all the observed intensities within of the observational uncertainties, with exception of the [S III]λ9069 + λ9532 and [O III]λ4363 emission lines, which are reproduced only for H 336 and NGC 5471-D; and for NGC 1170 and NGC 1176, respectively. Other works have also found that photoionization models are incapable of reproduce emission line intensities sensitive to $T_{\rm e}$ (e.g. Stasińska & Schaerer 1997; Oey et al. 2000). This problem has been atributted to temperature gradients and/or temperature inhomogeneities in nebulae which are not taken into account in simple photoionization models (see Stasińska 2002) such as the ones used in this paper. Because the [O III]λ4363 emission line has an exponential dependence on the electron temperature, any offset between the electron temperatures in photoionization models and observed forbidden-line temperatures will have the strong effect on the reproducion of this emission line.

5.1 Abundance determination comparison

To check the reliability of diagnostic diagrams, in Figs. 4 and 5 we present a comparison of O/H obtained from these methods with O/H abundances via $T_{\rm e}$-method and the difference among these estimations. We include in Fig. 5 the results of the detailed models for the H II regions in M 101 as well as the results of Pérez-Montero et al. (2010), who built detailed photoionization models in order to reproduce emission line intensities of 10 H II galaxies. In each plot, the average value ($\overline{\rm D}$) and the dispersion (σ) of this difference are also presented. The O/H and U values from the diagnostic diagrams were obtained by linear interpolation from the model grid shown in Fig. 2. In a few cases double values of Z and/or U for a same objects are found because the models overlap for a given combination of these parameter. For these, the estimations were not considered in our analysis. This happened mainly for the [N II]/Hα vs. [S II]/Hα diagnostic diagram (for about 5% of the points).

The diagnostic diagrams that provide the best results are the [O III]/[O II] vs. [N II]/[O II], [O III]/Hβ vs. [N II]/[O II], and ([O III]/Hβ)/([N II]/Hα) vs. [S II]/[S III], which give O/H estimates

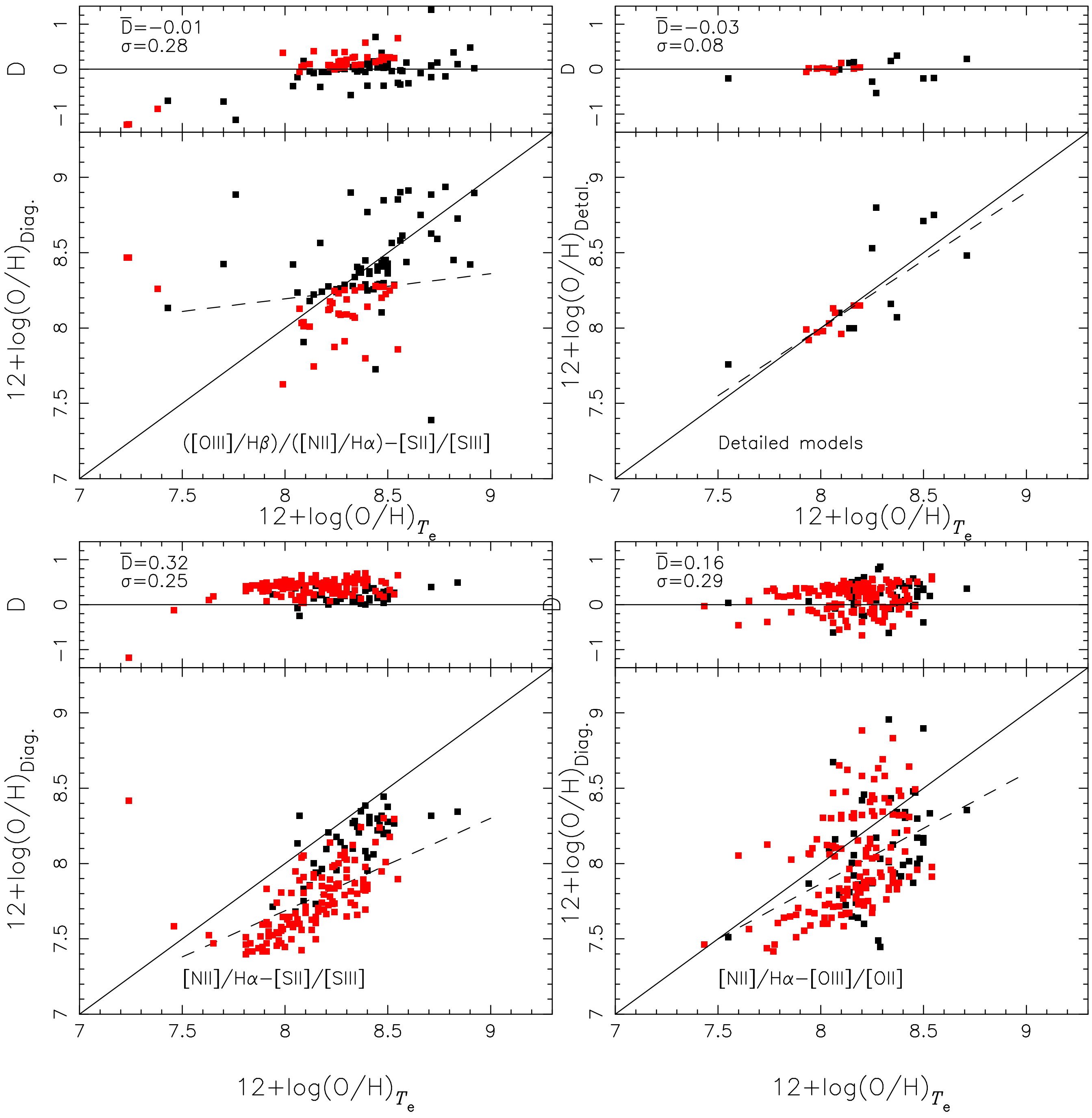

Figure 5. Same as Fig. 4, but for other diagnostic diagrams. The panel in the right top represents the comparison using detailed photoionization models and the red points were taken from Pérez-Montero et al. (2010).The results for H II galaxies and H II regions are indicated by different symbols (red and black dots, respectively).

close to the T_e-method with an absolute difference of about 0.04 dex. The lowest dispersion is found with the use of the [O III]/Hβ vs. [N II]/[O II] diagram. For the majority of the diagrams, the difference and the dispersion are larger in the regime of low metallicity (12+log(O/H)< 8.0). For the other diagrams this difference is about 0.25 dex. The O/H abundances via detailed models are in consonance with the ones via T_e-method for the objects analyzed and the dispersion derived is lower than the one obtained using diagnostic diagrams.

5.2 Ionization parameter determination

For the ionization parameter, in Fig. 6, we plotted U against the oxygen abundance obtained from diagnostic diagrams presented in Section 4 as well as those obtained from detailed models. The results for H II galaxies and H II regions are indicated by different symbols (red and black dots, respectively). The [O III]/Hβ vs. [N II]/[O II] and [O III]/[O II] vs. [N II]/[O II] estimates larger U values than the ones via other methods. There is not a clear trend of

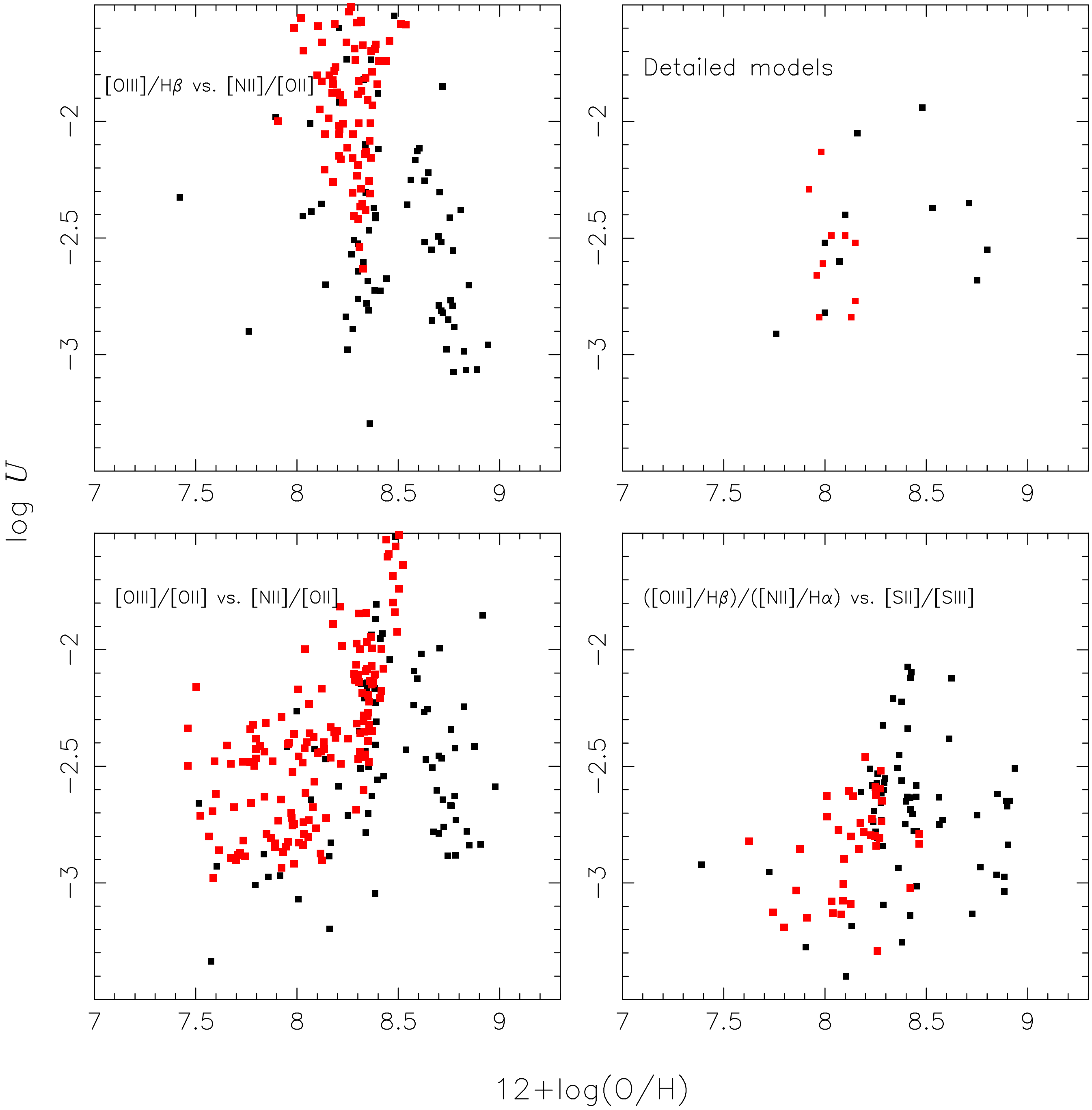

Figure 6. Logarithm of ionization parameter vs. oxygen abundances. Points represent the results using the diagnostic diagrams indicated in each plot. The results for H II galaxies and H II regions are marked by symbols with different colors (red for H II galaxies and black for H II regions). In the upper right plot the points represent estimations via detailed photoionization models, in which the red points were taken from Pérez-Montero et al. (2010).

U with O/H and this result is also confirmed by the detailed model estimation.

6 DISCUSSION

Comparing oxygen abundance determinations via T_e-method for the sample of H II regions and H II galaxies with those based on strong emission lines, we found that the [O III]/[O II] vs. [N II]/[O II], [O III]/Hβ vs. [N II]/[O II], and ([O III]/Hβ)/([N II]/Hα) vs. [S II]/[S III] diagnostic diagrams give O/H values nearest to the T_e-method, with differences of about 0.04 dex and a dispersion of about 0.30 dex. This difference is about the same as the one between oxygen estimates via the *P*-method (Pilyugin 2001) and via T_e-method found by López-Sanchez & Esteban (2010) considering a sample of Wolf-Rayet galaxies. It is lower by about 0.15 dex than the one found by these authors when using only one emission line ratio sensitive to metallicity.

As seen in Figs. 4 and 5, large difference are found for $12 + \log(O/H) < 8.0$ ($Z \lesssim 0.2\, Z_{\odot}$). Similar results were also found

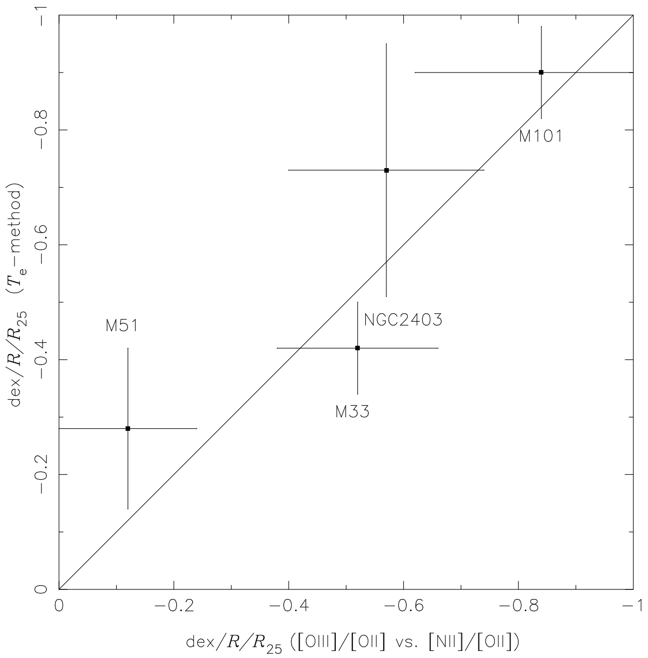

Figure 7. Comparison of abundance gradient slopes derived using the [O III]/[O II] vs. [N II]/[O II] and T_e-method for some galaxies as indicated. The slopes are measured in 12+log(O/H)/R/R_{25}, where R_{25} is the isophotal radius. The authors which we collected the gradients via T_e-method are cited in the text. Solid lines represent the equality of the two estimates.

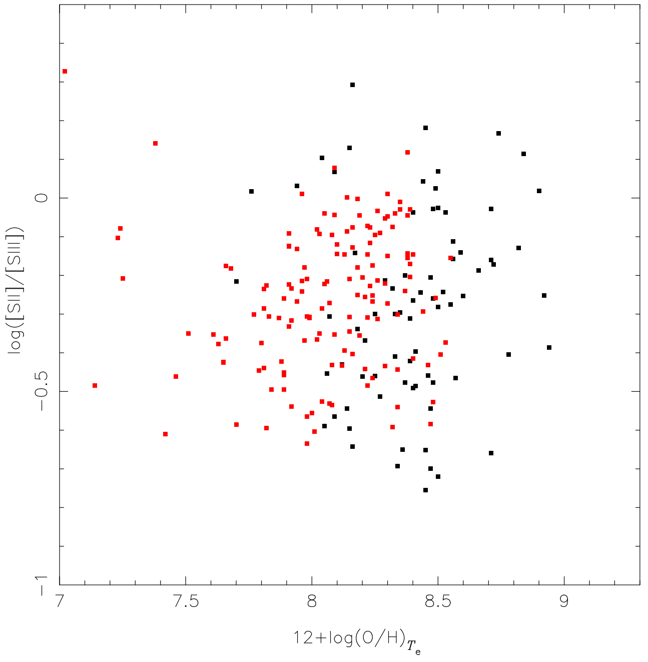

Figure 8. [S II]/[S III] line ratio observed versus oxygen abundance via T_e-method for our sample of objects. H II galaxies and H II regions are marked by red and black points, respectively.

by Yin et al. (2007), who compared oxygen estimates via N_2 and ([O III]/Hβ)/([N II]/Hα) with those via T_e-method for a sample of 695 galaxies and H II regions. This occurs because in this regime of metallicity the nitrogen and oxygen have both mainly a primary nucleosynthesis origin, doing nitrogen emission lines to be relatively independent on oxygen abundance and consequently the use of metallicity indicators based on these emission lines are not reliable. (e.g. Levesque et al. 2010; Dopita et al. 2000).

The origin of the dispersion found by us is probable due to the difference between the real N/O-O/H abundance relation of the object sample and the one assumed in our models. In fact, Pérez-Montero & Contini (2009) analyzed the dependence of N/O with O/H estimation obtained via the metallicity indicators using nitrogen line ratios and compared these estimations with the ones obtained via T_e-method. They found approximately the same dispersion as the one derived by us, and also showed that if the N/O ratio is taken into account in strong-line methods, the dispersion can be reduced by about 0.1 dex. Moreover, the scattering of N/O for a fixed O/H value is larger for the low metallicity regime (see e.g. Pilyugin et al. 2003), which introduces a larger dispersion for oxygen estimations in this regime, such as the one observed in our results. This is confirmed by the use of detailed models, for which the N/O-O/H relation is a free parameter, yielding a lower dispersion (0.08 dex) than the ones obtained from diagnostic diagrams. Yin et al. (2007) also obtained similar results comparing oxygen abundances derived from T_e-method and those via the photoionization models of Charlot & Longhetti (2001).

Another important test is to verify if abundance gradients estimates by using diagnostic diagrams agree with those via T_e-method. For that, in Fig. 7 we show a comparison of oxygen gradient slope computed using the [O III]/[O II] vs. [N II]/[O II] diagram presented in Fig. 2 and those via T_e-method for spiral galaxies M 101, M 51, M 33, and NGC 2403 obtained by Kennicutt et al. (2003), Bresolin et al. (2004), Magrini et al. (2007), and Garnett et al. (1997), respectively. We can see that, within the uncertainties given by the linear fitting, the diagnostic diagram above yields abundance gradient consistent with the ones via T_e-method. Again, the difference between the gradient estimates is probable due to the N/O-O/H relation assumed in our models and the one of the galaxies. This is supported by the detailed model results, since a linear fitting on oxygen abundance from these, presented in Table 2, yields a gradient for M 101 of 12+log(O/H)= 0.90(±0.26) R/R_{25} + 8.77(±0.15), the same gradients found by Kennicutt et al. (2003) using the T_e-method.

In general, oxygen determination obtained from strong-line methods, which use emission line intensities predicted by photoionization models, are overestimated up to 0.5 dex when compared with those obtained from T_e-method (Kewley & Ellison 2008; Dors & Copetti 2005; Kennicutt et al. 2003; Garnett et al. 2004; Stasińska 2002). This discrepancy is attributed to the fact that photoionization codes are not realistic enough, do not treat all the relevant physical processes correctly, use inaccurate atomic data, etc (Kennicutt et al. 2003). However, as seen previously, using the state of art of photoionization models and the combination of two line ratio, one sensitive to the metallicity and another sensitive to the ionization parameter, which does taken into account the physical conditions (hardness of the ionizing radiation and geometrical factor) of star-forming regions (Pilyugin 2001), minimizes the effects mentioned above and gives O/H estimates close to the T_e-method. As explained in Sect. 3, the match between solar abundances for the gas and star has little influence on metallicity indicators (i.e. [N II]/[O II]) showing that the metallicity estimates by our models are indepent of this fact.

The ionization parameter is expected to be dependent on the metallicity because stellar atmospheres of massive O stars become cooler with increasing metallicity as a result of enhanced line and wind blanketing (Massey et al. 2005), decreasing consequently the ionization parameter. Moreover, when stellar atmosphere abun-

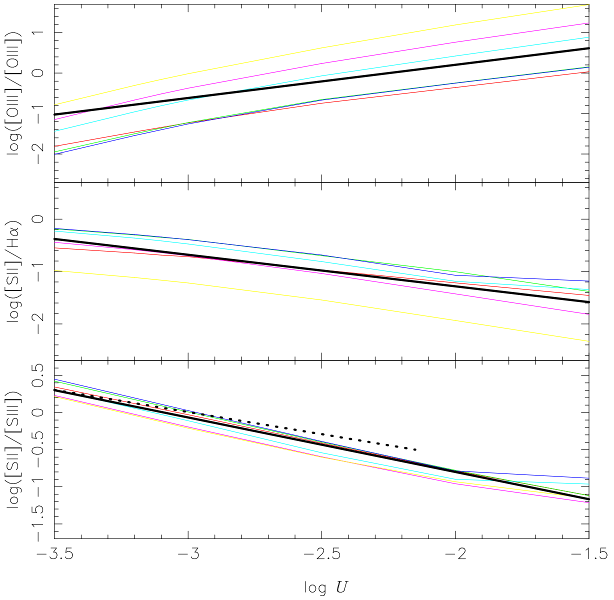

Figure 9. Relation between the ionization parameter *U* and the [S II]/[S III],[S II]/Hα and [O III]/[S II] line ratios. The colorful solid lines represent results for different metallicities, such as in Fig. 2, and the black solid line represents the linear fitting of the average of these results. The dotted line represents the relation proposed by Díaz et al. (1991).

dance is higher, this scatters the photons emitted from the photosphere more efficiently, causing a greater conversion efficiency from luminous energy flux to mechanical energy flux in the stellar wind base region, which also leads to a diminution of *U* in the H II region (Dopita et al. 2006). A decrease of *U* with the increase of *Z* was found for H II galaxies by Nagao et al. (2006) and Maier et al. (2006) and for disk H II regions by Bresolin et al. (1999). However, our results indicate no systematic dependency of the ionization parameter on the metallicity for the sample of objects considered, although using our grid of models it is impossible to check what factor (e.g. stellar effective temperature, geometrical factors, aging) is responsible for this behavior. This result is in consonance with the ones found by Dors & Copetti (2005), Garnett et al. (1997), and Kennicutt & Garnett (1996), who used the [S II]/[S III] in order to estimate the ionization parameter in H II regions located in spiral disks. To analyze whether our result is not an artefact of the methods used in this paper, in Fig. 8 we plotted the [S II]/[S III] line ratio intensity and the O/H abundances obtained by T_e-method of our sample. Again, we can note no systematic behavior of *U* with O/H.

As noted in Fig. 6, the [O III]/Hβ vs. [N II]/[O II] and [O III]/[O II] vs. [N II]/[O II] indicate very high *U* values ($\log U > -2$) for some objects, which are not predicted by the detailed model and by the ([O III]/Hβ)/([N II]/Hα) vs. [S II]/[S III] diagram. This occurs because photoionization models underpredict the [O III]/Hβ (see Fig. 2), mainly for objects with low metallicity. Because these line ratios are age dependent, it is possible that models assuming a harder spectral energy distribution would resolve this problem. Thus, we ran a grid of photoionization models (not shown) using as ionizing source a cluster of 1 Myr and computed *U* and *Z* values. We found that, for the diagram with [O III]/[O II], this new grid yields values of *U* in consonance with the ones from other diagrams. However, for the diagram with [O III]/Hβ, although a better match between the models and the observational data was obtained, the *U* estimations continue to be overestimated in relation to the ones via other methods. The O/H estimates practically did not change in these cases. A similar problem was also pointed out by Stasińska & Izotov (2003), who using a sequence of photoionization models to reproduce observational data of H II galaxies, which found that the models underpredict [O III]/Hβ for objects with $7.4 < \log(\mathrm{O/H}) < 8.0$. These authors invoked several mechanisms to explain this discrepancy, such as secondary ionization by X-rays and shocks but a definitive conclusion was not reached. Recently, Levesque et al. (2010) compared observational data of a large sample of star-forming galaxies with grid of photoionization models, such as the ones presented in this paper, but considering as ionizing source stellar cluster with different ages and formed by instantaneous and continuous star formation. Similar to our results, they found that very young models with 0-1 Myr and formed instantaneously reproduce better the observed [O III]/Hβ than the older ones, although better agreement is given by models adopting a continuous star formation history (see also Pérez-Montero et al. 2010). These authors did not compare *U* estimates obtained by different emission line ratio, but it is probable that the discrepancy found by us is maintained even using their models with continuous star formation. Levesque et al. (2010) showed that the new generation of Geneva evolutionary tracks, which include stellar rotation, produces a SED more prominent in the higher-energy regime ($\lambda \lesssim 230$ Å) than the one used here, with rotation effects being more important at lower metallicity. Thus, it is probable that if these SEDs were used in our photoionization models, the predicted intensities of the [O III]/Hβ would be larger and *U* estimates from diagnostic diagrams using this line ratio would conciliate with the ones from other diagrams.

As the [S II]/[S III] ratio is weakly dependent on *Z*, it is useful to calibrate it with *U*. In Fig. 9, we show the *U*-[S II]/[S III] relation predicted by our models for the entire range of *Z* and the relation proposed by Díaz et al. (1991), as well as our results for [S II]/Hα and [O III]/[O II] versus *U*.

A linear fitting of the average of these photoionization model results produce

$$\log U = -1.36\,(\pm 0.07)\log[\mathrm{S\,II}]/[\mathrm{S\,III}] - 3.09\,(\pm 0.05), \tag{1}$$

$$\log U = -1.66\,(\pm 0.06)\log[\mathrm{S\,II}]/\mathrm{H}\alpha - 4.13\,(\pm 0.07), \tag{2}$$

$$\log U = 1.22\,(\pm 0.07)\log[\mathrm{O\,II}]/[\mathrm{O\,III}] - 2.25\,(\pm 0.05). \tag{3}$$

As can be seen in Fig. 9, the [S II]/Hα is a good *U* indicator because it shows little variation with the metallicity for $Z > 0.2\,Z_\odot$ and uses emission line with near wavelength, being almost independent of the reddening. Our result for *U*-[S II]/[S III] relation is in very good agreement with the relation proposed by Díaz et al. (1991).

7 CONCLUSION

We compared oxygen estimates for a large sample of objects obtained by direct detection of the electron temperature with those via diagnostic diagrams containing strong emission lines predicted by photoionization models, as well as from detailed models. Among the diagnostic diagrams considered, we found that the ones utilizing the emission lines [O III]/[O II] vs. [N II]/[O II], [O III]/Hβ vs. [N II]/[O II], and [O III]/Hβ/[N II]/Hα vs. [S II]/[S III] diagnostic diagrams give O/H values nearest to the T_e-method, with differences of about 0.04 dex and dispersion of 0.3 dex. Similar results were obtained using detailed models but with a smaller dispersion, of 0.08 dex. The origin of the dispersion is probably due to differences between the real N/O-O relation of the sample and the one assumed in the models. We did not find any correlation of the ionization parameter with the metallicity for the objects in our sample. We conclude that the combination of two line ratio predicted by photoionization models, one sensitive to the metallicity and another sensitive to the ionization parameter, which does taken into account the physical conditions of star-forming regions, gives O/H estimates close to the values derived using direct detections of electron temperatures.

ACKNOWLEDGEMENTS

This work was supported by FAPESP under grant 2009/14787-7. GH is grateful to the Spanish *Ministerio de Educación y Ciencia* for support under grant AYA2007-67965-C03-03 and AYA2010-21887-C04-03, and the Comunidad de Madrid under grant S2009/ESP-1496 (ASTROMADRID). EPM is grateful to the Spanish *Ministerio de Ciencia e Innovación* for support under grant AYA2007-67965-C03-02 and AYA2010-21887-C04-02, and the Junta de Andalucía under grant TIC114.

REFERENCES

Allende Prieto, C., Lambert, D. L., Asplund, M. 2001, ApJ, 556, 63L
Alloin, D., Collin-Souffrin, S., Joly, M., Vigroux, L. 1979, A&A, 78, 200
Baldwin, J. A., Phillips, M. M., Terlevich, R. 1981, PASP, 93, 5
Bresolin, F., Gieren, W., Kudritzki, R. et al. 2009, ApJ, 700, 309
Bresolin, F. 2007, ApJ, 656, 186
Bresolin, F., Schaerer, D., González Delgado, R. M., Stasińska, G. 2005,A&A, 441, 981
Bresolin, F., Garnett, D. R., Kennicutt, R. C., 2004, 615, 228
Bresolin, F., Kennicutt, R. C., Garnett, D. R. 1999, ApJ, 510, 104
Charlot, S, & Longhetti, M. 2001, MNRAS, 323, 887
Copetti, M. V. F., Mallmann, J. A. H., Schmidt, A. A., Castañeda, H. O. 2000, A&A,357,621
Copetti, M. V. F., Pastoriza, M. G., Dottori, H. A. 1986, A&A, 156, 111
Copetti, M. V. F., Pastoriza, M. G., Dottori, H. A. 1985, A&A, 152, 427
Díaz, A. I., & Pérez-Montero, E. 2000, MNRAS, 312, 130
Díaz, A. I., Terlevich, E., Castellanos, M., Hägele, G. F. 2007, MNRAS, 382, 251
Díaz, A. I., Terlevich, E., Vílchez, J. M., Pagel, B. E. J., Edmunds, M. G. 1991, MNRAS, 253, 245
Dopita, M. A., Fischera, J., Sutherland, R. S. 2006, 2006, ApJS, 167, 177
Dopita, M. A., Kewley, L. J., Heisler, C. A., Sutherland, R. S. 2000, ApJ, 543, 224
Dopita, M. A., & Evans, I. N. 1986, ApJ, 307, 431
Dors, O. L., Storchi-Bergmann, T., Riffel, R. A., Schimdt, A. A. 2008, A&A, 482, 59
Dors, O. L., & Copetti, M. V. F., 2006, A&A, 452, 437
Dors, O. L., & Copetti, M. V. F., 2005, A&A, 437, 837
Dors, O. L., & Copetti, M. V. F., 2003, A&A, 404, 969
Edmunds, M. G., & Pagel, B. E. J. 1984, MNRAS, 211, 507
Ellison, S. L., Patton, D. R., Simard, L. et al. 2010, astroph/1002.4418
Evans, I. N. 1986, ApJ, 309, 544
Fernandes, R. C., Leão, J. R. S., Lacerda, R. R. 2003, MNRAS, 340, 29
Ferland, G. J. 2002, Hazy, a brief introduction to Cloudy 96.03, Univ. Kentucky, Dept. Phys., Astron. internal report
Garnett, D. R., Edmunds, M. G., Henry, R. B. C., Pagel, B. E. J., Skillman, E. D. 2004, AJ, 128, 2772
Garnett, D. R., Shields, G. A., Skillman, E. D., Sagan, S. P., & Dufour, R. J. 1997, ApJ, 489, 63
Garnett, D. R., Dufour, R. J., Peimbert, M., et al. 1995, ApJ, 449, 77
Garnett, D. R. 1989, ApJ, 345, 282
Grevesse, N., & Sauval, A. 1998, Space Sci. Rev., 85, 161
Garca-Vargas, M. L., Bressan, A., Díaz, A. I. 1996, A&AS, 112, 13
Gavilń, M., Buell, J. F.; Mollá, M. 2005, A&A, 432, 861
Guseva, N. G., Izotov, Y. I., Thuan, T. X. 2000, 531, 776
Izotov, Y. I., Stasińska, G., Meynet, G., Guseva, N. G., Thuan, T. X. 2006, A&A, 448, 955
Izotov, Y. I., & Thuan, T. X. 2004, ApJ, 602, 200
Hägele, G. F., Díaz, A. I., Terlevich, E., Terlevich, R., Pérez-Montero, E., Cardaci, M. V. 2008, MNRAS, 383, 209
Kennicutt, R. C., Bresolin, F., Garnett, D. R. 2003, ApJ, 591, 801
Kennicutt, R. C., Jr., & Garnett, D. R. 1996, ApJ, 456, 504
Kewley, L. J., Rupke, D., Jabran Zahid, H., Geller, M. J., Barton, E. J. 2010, astroph/1008.2204
Kewley, L. J., & Ellison, S. L 2008, ApJ, 681, 1183
Kewley, L. J., & Dopita, M. A. 2002, ApJS, 142, 35
Kewley, L. J., Dopita, M. A., Sutherland, R. S., Heisler, C. A., Trevena, J. 2001, ApJ, 556, 121
Kobulnicky, H. A., Kennicutt, R. C., Pizagno, J. L. 1999, ApJ, 514, 544
Krabbe, A. C., Pastoriza, M. G., Winge, C., Rodrigues, I., Ferreiro, D. L. 2008, MNRAS, 389, 1593
Krabbe, A. C., Rembold, S. B., Pastoriza, M. G. 2007, MNRAS, 378, 569
Kunth, D., & Sargent, W. L. W. 1983, ApJ, 273, 81
López-Sanchez, A. R., & Esteban, C. 2010, astroph/1004.5251
Lee, H., & Skillman, E. D. 2004, ApJ, 614, 698
Lee, J. C., Salzer, J. J., Melbourne, J. 2004, ApJ, 616, 752
Leitherer, C., Schaerer, D., Goldader, J. D. et al. 1999, ApJS, 123, 3
Levesque, E. M., Kewley, L. J., Larson, K. L. 2010, AJ, 139, 712
Liang, Y. C., Hammer, F., Yin, S. Y., Flores, H., Rodrigues, M.,Yang, Y. B. 2006, A&A, 473, 411
Maier, C., Lilly, S. J., Carollo, C. M., et al. 2006, ApJ, 639, 858
Magrini, L., Vílchez, J. M., Mampaso, A., Corradi, R. L. M., Leisy, P. 2007, A&A, 470, 865
Martín-Manjón, M. L., Mollá, M., Díaz, A. I., Terlevich, R. 2008, MNRAS, 385, 854
Massey, P., Puls, J., Pauldrach, A. W. A., Bresolin, F., Kudritzki, R. P., Simon, T. 2005, ApJ, 627, 477
Mazzuca, L. M., Sarzi, M., Knapen, J. H., Veilleux, S., Swaters, R. 2006, ApJ, 649, L79
Mayya, Y. D., Prabhu, T. P. 1996, AJ, 111, 1252
McGaugh, S. 1991, ApJ, 380, 140
Meynet, G., Maeder, A., Schaller, G., Schaerer, D., Charbonnel, C. 1994, A&AS, 103, 97
Mollá, M., & Díaz, A. I. 2005, MNRAS, 358, 521
Nagao, T., Maiolino, R., Marconi, A. 2006, A&A, 459, 85
Oey, M. S., Dopita, M. A., Shields, J. C., Smith, R. C. 2000, ApJS, 128, 511
Pagel, B. E. J., Edmunds, M. G., Blackwell, D. E., Chun, M. S., Smith, G. 1979, MNRAS, 189, 95

Pauldrach, A. W. A., Hoffmann, T. L., Lennon, M. 2001, A&A, 375, 161
Pettini, M., Pagel, B.e dependence of the calibration of the N2 parameter on the N/O ra E. J. 2004, MNRAS, 348L, 59
Pérez-Montero, E., García-Benito, R., Hägele, G. F. Díaz, A. I. 2010, MNRAS, 404, 2037
Pérez-Montero, E., & Contini, T. 2009, MNRAS, 398, 949
Pérez-Montero, E., Díaz, A. I., Vílchez, J. M., Kehrig, C. 2006, A&A, 449, 193
Pérez-Montero, E., Díaz, & A. I. 2005, MNRAS, 361, 1063
Pilyugin, L. S., Contini, T., Vílchez, J. M. 2004, A&A, 423, 427
Pilyugin, L. S., Vílchez, J. M., Contini, T. 2004, A&A, 425, 849
Pilyugin, L. S., Thuan, T. X., Vílchez, J. M. 2003, A&A, 397, 487
Pilyugin, L. S. 2001, A&A, 369, 594
Rupke, D. S. N., Veilleux, S., Baker, A. J. 2008, ApJ, 674, 172
Stanghellini, L., Magrini, L., Villaver, E. Galli, D. 2010, astroph/1006.4076
Skillman, E.D., Kennicutt, R. C., Shields, G. A., Zaritsky, D. 1996, ApJ, 462, 147
Stasińska, G., & Izotov, I. 2003, A&A, 397, 71
Stasińska, G. 2002, in Revista Mexicana de Astronomia y Astrofisia Conference Series, 12, 62
Stasińska, G., & Schaerer, D. 1999, A&A, 351, 72
Stasińska, G., & Schaerer, D. 1997, A&A, 322, 615
Storchi-Bergmann, T., Calzetti, D., & Kinney, A. L. 1994, ApJ, 429, 572
van Hoof, P. A. M., Weingartner, J. C., Martin, P. G., Volk, K., & Ferland, G. J. 2001, in Challenges of Photoionized Plasmas, ed. G. Ferland & D. Savin (San Francisco: ASP), ASP Conf Ser., 247, 363
Vílchez, J. M., & Iglesias-Páramo, J. 2003, ApJS, 145, 225
Vílchez, J. M., Esteban, C. 1996, MNRAS, 280, 720
Vila-Costas, M. B., & Edmunds, M. G. 1993, MNRAS, 265, 199
Viironen, K.; Delgado-Inglada, G.; Mampaso, A.; Magrini, L.; Corradi, R. L. M. MNRAS, 381, 1719
Yin, S. Y., Liang, Y. C., Hammer, F., Brinchmann, J., Zhang, B., Deng, L. C., Flores, H. 2007, A&A, 462, 535
Zaritsky, D, Kennicutt, R C., Huchra, J. P. 1994, ApJ, 420, 87